Microwave Engineering
Ulm University

universität ulm

A Broadband Multilayer Vertical Transition at 79 GHz Employing FR4 as Core Material

Dominik Schwarz, Nico Riese, André Dürr, Christian Waldschmidt

European Microwave Week 2021 Conference Proceedings.
DOI: 10.23919/EuMC50147.2022.9784202

A Broadband Multilayer Vertical Transition at 79 GHz Employing FR4 as Core Material

Dominik Schwarz[1], Nico Riese, André Dürr, and Christian Waldschmidt
Institute of Microwave Engineering, Ulm University, 89081 Ulm, Germany
[1]dominik-1.schwarz@uni-ulm.de

***Abstract* — A novel vertical transition through a multilayer printed circuit board is presented. The transition is designed to fulfill the cost and manufacturing constraints of next generation automotive radar sensors. This is achieved both by employing FR4 as material in the transition core and the fabrication in a standard high density interconnect process. The modified design of a quasi-coaxial structure solves the limitations determined by the constraints. Although FR4 has high dielectric losses, a vertical transition through multiple FR4 layers is realized with a low insertion loss of less than 2.1 dB within the automotive radar frequency range of 76 GHz to 81 GHz. A return loss better than 10 dB is achieved up to a frequency of 83.2 GHz. The reliability and repeatability of the transition is shown by measurements of several transitions from different production cycles.**

***Keywords* — E-band, high density interconnect, mm-wave, multilayer, printed circuit board, quasi-coaxial structure, stripline, vertical transition, via transition.**

I. Introduction

Future driver assistance systems and the development of autonomous driving require radar sensors with a high detection performance and high-resolution capabilities in range and angle. In order to enable 2-dimensional beamforming, a large number of hardware channels is needed, while adhering cost and size restrictions [1], [2]. Therefore, a highly flexible antenna placement must be allowed on the carrier board, which requires a signal distribution concept on multiple mm-wave signal layers. For the next generation of sensors, this can only be achieved by means of low-loss and cost-effective vertical transitions.

In multilayer designs, simple transitions using only three vias as in [3] are not sufficient. State-of-the-art vertical transitions for highly complex boards in low temperature cofired ceramics (LTCC) imitate coaxial lines and have superior performance [4], but are very costly. Similar transitions can be realized in an radio frequency (RF) printed circuit board (PCB) with reduced costs but higher losses [5].

An obvious way to further reduce costs is to replace RF substrates by conventional PCB materials. However, the loss in performance is typically too large. One way to retain the low losses is to manufacture only a metallized ground cavity in a low-cost PCB that forms the outer conductor of a coaxial line. Afterwards, a polytetrafluoroethylene (PTFE) bush as low loss dielectric and a signal pin are inserted to realize a true coaxial structure [6]. This technology comes with a high assembly complexity and is therefore not feasible for an increasing number of hardware channels.

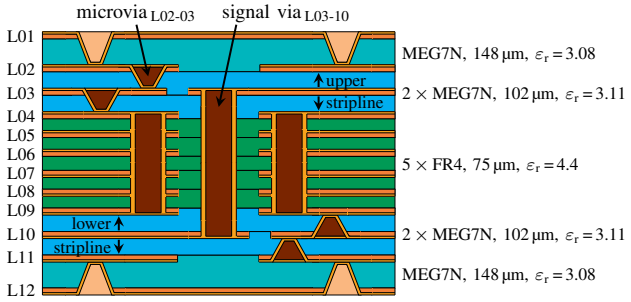

Fig. 1. Cross section of the multilayer PCB.

In this work, we present a novel broadband vertical transition, which is fabricated in a standard high density interconnect (HDI) process and employs FR4 as core material. Multiple mm-wave, digital, and power layers enable the design of complex sensors. The realized vertical transition is robust to deviations from the assumed permittivity and achieves low losses despite the usage of FR4.

II. Design and Fabrication

The utilization of glass-based RF-substrate materials in combination with FR4 facilitates the application of a standard HDI process. Copper losses in the RF layers are reduced by means of the ultra-flat copper foil BF-TZA. In the outer layers, a thicker substrate is used to improve the radiation efficiency of the antennas. The complete layer stack is depicted in Fig. 1. In the following, the design procedure of the transition between the lower and upper stripline as depicted in Fig. 2 is introduced.

A. Hardware Constraints

To keep manufacturing costs low, standard drill sizes of 0.2 mm, microvias with an aspect ratio of 1, and only staggered microvias are used. A minimum spacing of 100 µm is met. The transition is designed to be repeated on a 1.3 mm grid, which fits to the pitch of standard ball grid array packages of state-of-the-art radar integrated circuits [7].

B. Quasi-Coaxial Structure

The main element of the vertical transition is a quasi-coaxial structure in FR4 from layer L04 to L09. A small diameter of the signal pin and a high number of surrounding vias have been shown to improve the performance at higher frequencies [8]. The introduced concept of realizing

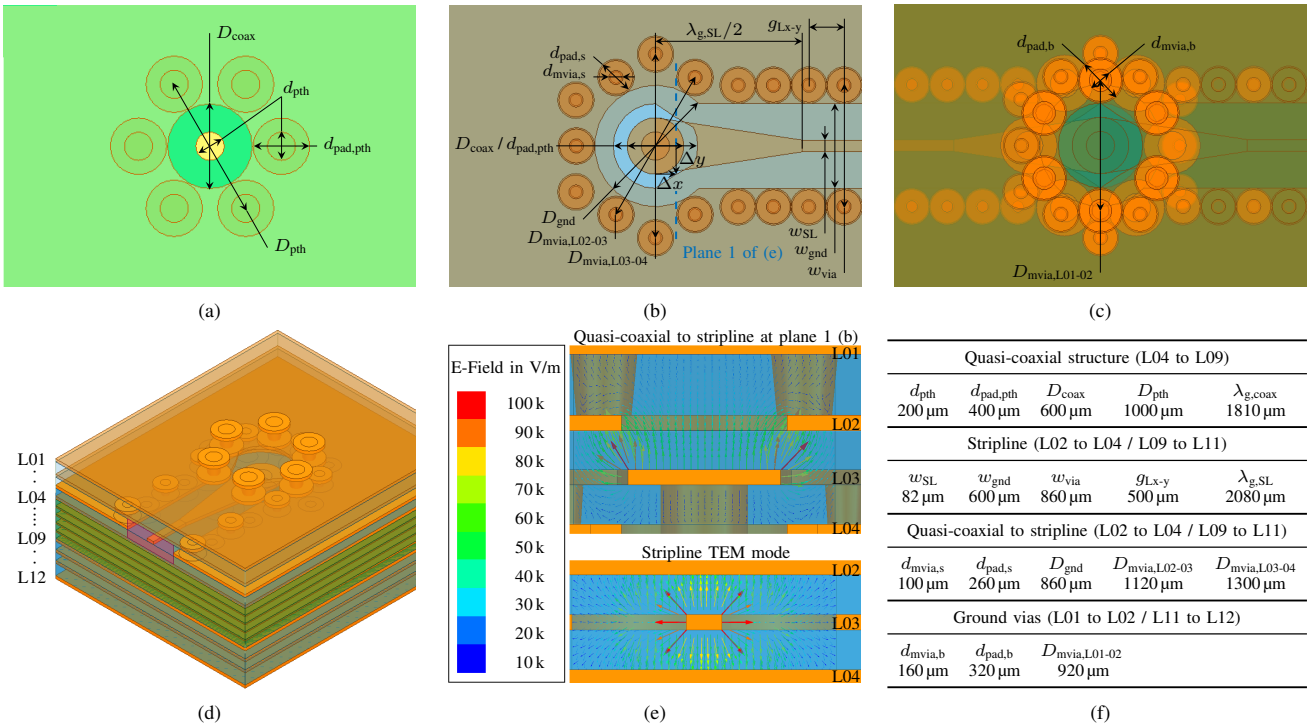

Quasi-coaxial structure (L04 to L09)				
d_{pth}	$d_{pad,pth}$	D_{coax}	D_{pth}	$\lambda_{g,coax}$
200 µm	400 µm	600 µm	1000 µm	1810 µm
Stripline (L02 to L04 / L09 to L11)				
w_{SL}	w_{gnd}	w_{via}	$g_{Lx\text{-}y}$	$\lambda_{g,SL}$
82 µm	600 µm	860 µm	500 µm	2080 µm
Quasi-coaxial to stripline (L02 to L04 / L09 to L11)				
$d_{mvia,s}$	$d_{pad,s}$	D_{gnd}	$D_{mvia,L02\text{-}03}$	$D_{mvia,L03\text{-}04}$
100 µm	260 µm	860 µm	1120 µm	1300 µm
Ground vias (L01 to L02 / L11 to L12)				
$d_{mvia,b}$	$d_{pad,b}$	$D_{mvia,L01\text{-}02}$		
160 µm	320 µm	920 µm		

(f)

Fig. 2. Sketch of the optimized vertical transition: (a) top view on the quasi-coaxial structure layers in FR4 (L04 to L09); (b) top view on the quasi-coaxial-to-stripline transition layers (L02 to L04, point symmetric on L09 to L11); (c) top view on all layers (L01 to L10); (d) 3-dimensional view, the layers L01 and L02 are semi-transparently drawn; (e) vectorial electromagnetic field plots demonstrating the electromagnetic behavior at the transition between the stripline and the quasi-coaxial structure; (f) dimensions of the optimized and fabricated structure.

the signal via L03-10 without restrings in the interjacent layers is advantageous, since a narrower signal pin diameter can be realized. In addition, the structure is more similar to an ideal coaxial line, as only the return path is ragged. The latter is realized with six surrounding buried ground vias, leaving enough space to stagger six corresponding microvias in the subsequent RF-substrates. A top view on the quasi-coaxial element is shown in Fig. 2 (a) with the dimensions in (f).

As the layer thickness is below a twentieth of the guided wavelength, thickness tolerances in the FR4-substrates influence only the length and therefore the insertion loss of the transition. The effective cross section and the characteristic impedance remain unchanged, and hence the return loss.

An approximation for the upper frequency limit is the cutoff frequency f_{cutoff} of the TE_{11} mode in coaxial lines, which is given by [9]

$$f_{cutoff,TE_{11}} \approx \frac{c_0}{\pi\sqrt{\varepsilon_r}\cdot(d_{pth}+D_{coax})/2}\,, \tag{1}$$

with the speed of light c_0, the relative permittivity ε_r, the inner diameter d_{pth}, and the outer diameter D_{coax}. For the given structure, this results in 114 GHz, which is significantly above the desired operating frequency range.

In Fig. 3 (- - -) the performance degradation caused by the usage of restrings on all layers with respect to the optimized structure (——) is shown. This results in significantly larger losses and a narrowband match shifted to higher frequencies.

Typically, FR4 material is affected by deviations from the nominal permittivity. A variation of ±10 % shows only a small impact on the performance, see Fig. 3 (-·-·-) and (- · -). The insertion loss increases by a maximum of 0.4 dB, while the lower $|S_{11}| < -10$ dB-frequency increases by only 2 GHz with an unchanged upper frequency limit.

C. *Quasi-Coaxial-to-Stripline Transition*

A tapered feed line and anti-pads in the subsequent layers compensate mismatches in the transition between the stripline and the quasi-coaxial structure [10]. As depicted in Fig. 2 (b), a taper with a length of $\lambda_{g,SL}/2$ is introduced in layer L03 to improve matching. The typically circular anti-pads are trimmed on both sides according to the quadratic term

$$\Delta y = \frac{D_{coax}/2}{w_{par}^2}\cdot(w_{par}-\Delta x)^2\,, \tag{2}$$

for $0 \le \Delta_x \le 270$ µm and the parable width $w_{par} = 800$ µm from the signal via midpoint in direction to the stripline. This improves the transition from the stripline mode to the coaxial TEM mode, as the field is concentrated between the upper stripline edges and the trimmed anti-pad, see Fig. 2 (e). Subsequently, the field is guided above the signal pad into the coaxial mode. The return loss deteriorates at higher frequencies when standard circular anti-pads are used, see Fig. 3 (- -).

The microvias L02-03 in the return path have the same x and y coordinates as the buried plated through holes (PTH)

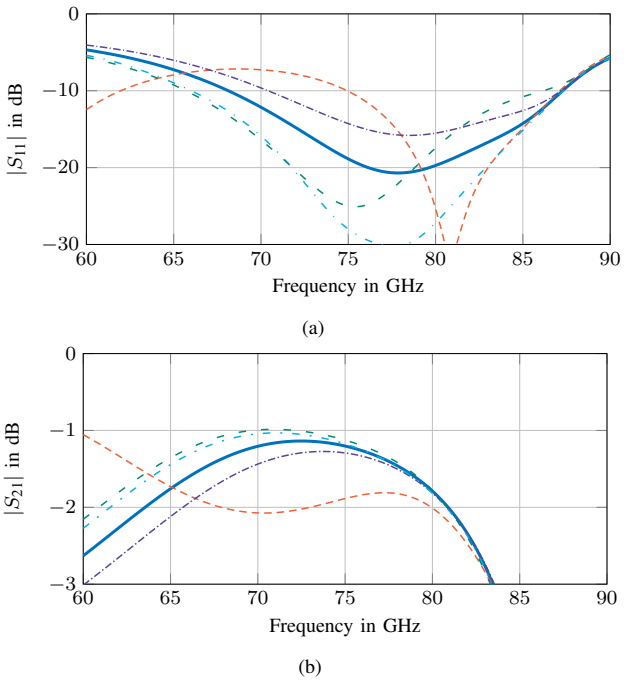

Fig. 3. Simulation results of the optimized and fabricated vertical stripline-to-stripline transition through FR4 (——) with respect to the influence of restrings in the signal via on all layers (– – –), the influence of a by 10 % decreased (–·–·–) or increased (– · · –) permittivity of the FR4 material and the influence of omitting the quadratic trimming of the anti-pad in the quasi-coaxial-to-stripline transition (– –): (a) $|S_{11}|$; (b) $|S_{21}|$.

in the quasi-coaxial structure. The microvias L03-04 are staggered in-between at a wider diameter fitting the repetition grid.

D. Overall Transition and Fabrication

The overall transition is a combination of the quasi-coaxial structure and two quasi-coaxial to stripline transitions, see Fig. 2 (d). To prevent unwanted radiation, the structure is finished with outer ground layers, that are connected with a microvia ring as depicted in Fig. 2 (c). While the insertion loss of the optimized structure is limited by the dielectric losses in the FR4 core, the maximum operating frequency is limited by the hardware constraints (cf. section II-A).

A precise manufacturing of the optimized structure is possible with the used standard HDI process, which is demonstrated by a micrograph of the manufactured transition as shown in Fig. 4.

III. Stripline-to-Microstrip Transition

To enable measurements of the vertical transition, an additional stripline-to-microstrip transition is designed. Two staggered microvias are used, as no direct via between the layers L01 and L03 is available. Both microvias are connected with a connection line (CL) in layer L02. The key element of this transition is the elliptical anti-pad in L02, as depicted in Fig. 5. The matching is improved using a taper from the signal microvia L02-03 to the stripline width w_{SL}.

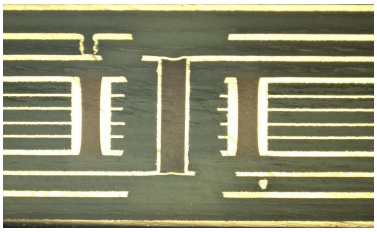

Fig. 4. Example micrograph of the manufactured vertical transition.

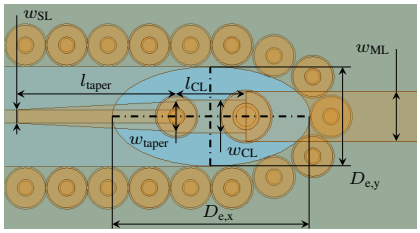

(a)

w_{CL}	200 µm
l_{CL}	420 µm
$D_{\mathrm{e,x}}$	1200 µm
$D_{\mathrm{e,y}}$	600 µm
l_{taper}	960 µm
w_{taper}	180 µm
w_{SL}	82 µm
w_{ML}	300 µm

(b)

Fig. 5. Sketch of the stripline-to-microstrip transition. All microvia dimensions and the microvia fence beneath the stripline correspond to the vertical transition (cf. Fig. 2): (a) top view on the transition layers L01 to L03 and (b) dimensions of the optimized and fabricated structure.

IV. Measurement Results

Multiple structures from different production cycles are measured to obtain a reliable validation of the vertical transition. The measurements are performed with mm-wave probes, see Fig. 6. Since it is only possible to probe from one side, back-to-back structures are employed. Therefore, two identical transitions are connected with a thru and a line standard in-between, respectively. From measurements of both configurations the scattering parameters of a single transition can be calculated [3]. The calibration of the network analyzer is performed with thru-reflect-line (TRL) calibration kits in the microstrip and the stripline plane.

First, the performance of the stripline-to-microstrip transition is evaluated. As can be seen in the measurement results shown in Fig. 7, a broadband match is realized with an $|S_{11}|$ of less than −14 dB over the whole E-band. The measured insertion loss is 0.75 dB at 79 GHz. Despite the deviations from the simulation, only small variations occur between the measurements of all transitions. This proves that the later performed calibration in the stripline plane is valid for all measurements.

The measured insertion and return loss of the vertical transition coincides well with the simulation, see Fig. 8. Again, only minor variations occur between all 48 measurements. An

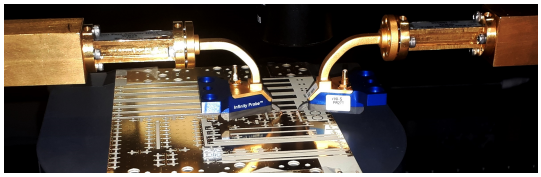

Fig. 6. Photograph of the measurement setup.

Table 1. Comparison to other vertical transitions. Maximum frequency and loss are taken from measurement curves at the $|S_{11}| < -10\,\text{dB}$-bandwidth.

Source	f_{max}	Max. loss	Transition height	Vertical transition type	Assembly complexity	Cost
[6]	>18 GHz	0.3 dB	0.9 mm	True coaxial with PTFE bush and signal pin	high	medium
[4]	>70 GHz	0.6 dB	0.9 mm	Quasi-coaxial structure in LTCC	low	high
[5]	71.5 GHz	2.0 dB	1.0 mm	Between PCBs with excavated structure	medium	medium
This work	83.2 GHz	2.3 dB	0.8 mm	Multilayer HDI-PCB with FR4 core	low	low

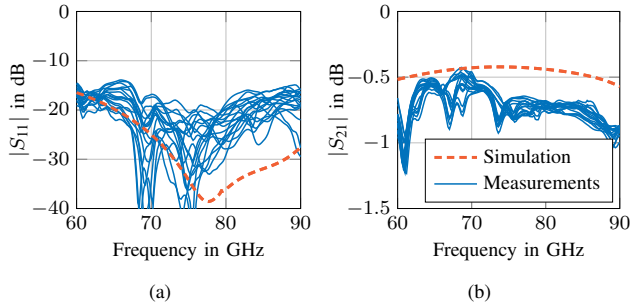

(a) (b)

Fig. 7. Measurement results of 18 fabricated stripline-to-microstrip transitions in comparison to the simulation: (a) $|S_{11}|$; (b) $|S_{21}|$.

$|S_{11}|$ value of less than −10 dB is realized for all transitions in a frequency range between 70.5 GHz and 83.2 GHz. This significantly exceeds the operating frequency range of state-of-the-art radar transceivers (76 GHz to 81 GHz [7]). The insertion loss in the latter range is between 1 dB and 2.1 dB. For the upper frequency limit the maximum measured insertion loss of 2.4 dB is even 0.5 dB lower than simulated.

V. Comparison to the State-of-the-Art

In Tab. 1 the key parameters of the proposed vertical transition are compared to other presented transitions. The insertion loss of the proposed transition through an FR4 core is comparable to other transitions in multilayer PCBs. Lower losses or higher frequencies can only be achieved at the cost of a higher assembly complexity or higher fabrication costs. In summary, the presented transition is the most cost-effective and achieves a low insertion loss.

VI. Conclusion

In this paper, we showed that cost-effective vertical transitions at 79 GHz can be realized in complex multilayer PCBs with an FR4 core. Therefore, the transitions were fabricated in a standard HDI process. The reliability and repeatability was proven by measurements of several transitions from different production cycles. A maximum frequency of 83.2 GHz has been achieved for a return loss better than 10 dB. The transition has a low insertion loss of less than 2.1 dB in the whole automotive radar frequency range from 76 GHz to 81 GHz, which enables the simplified and cost-effective realization of next generation automotive radar sensors.

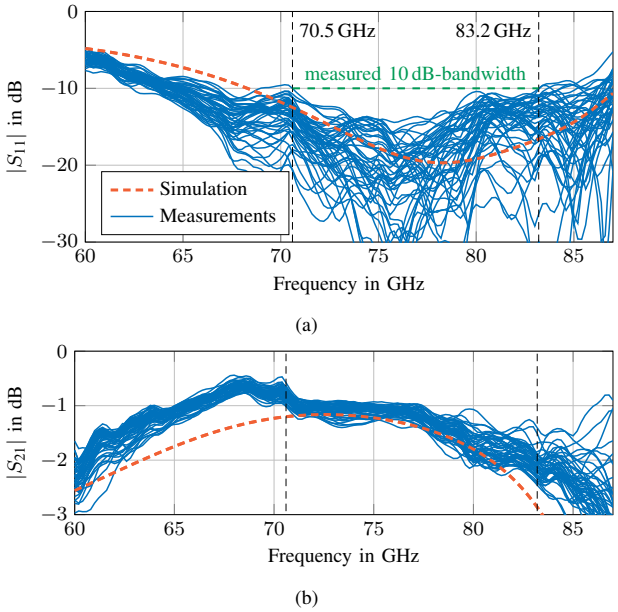

(a) (b)

Fig. 8. Measurement results of 48 fabricated vertical transitions through FR4 in comparison to the simulation performed using a high loss model to provide an upper bound on the expected loss: (a) $|S_{11}|$; (b) $|S_{21}|$.

References

[1] J. Hasch, "Driving Towards 2020: Automotive Radar Technology Trends," in *IEEE MTT-S International Conference on Microwaves for Intelligent Mobility (ICMIM)*, Apr. 2015, pp. 1–4.

[2] C. Waldschmidt, J. Hasch, and W. Menzel, "Automotive Radar — From First Efforts to Future Systems," *IEEE Journal of Microwaves*, vol. 1, no. 1, pp. 135–148, Jan. 2021.

[3] T. Galler, T. Chaloun *et al.*, "Hermetically Sealed Glass Package for Highly Integrated MMICs," in *49th European Microwave Conference (EuMC)*, Oct. 2019, pp. 292–295.

[4] C. Tsai, Y. Cheng, T. Huang *et al.*, "Design of Microstrip-to-Microstrip Via Transition in Multilayered LTCC for Frequencies up to 67 GHz," *IEEE Transactions on Components, Packaging and Manufacturing Technology*, vol. 1, no. 4, pp. 595–601, Apr. 2011.

[5] S. Yoshida and K. Nishikawa, "Experimental Verification of Excavated Structure on Multi-Layered Substrates for Millimeter-Wave Signal Vertical Transition Using Copper Balls," *IEEE Access*, vol. 8, pp. 2362–2372, Jan. 2020.

[6] G. Anand, R. Lahiri, and R. Sadhu, "Wide Band Microstrip to Microstrip Vertical Coaxial Transition for Radar & EW Applications," in *Asia-Pacific Microwave Conference (APMC)*, Dec. 2016, pp. 1–4.

[7] B. P. G. et al, "A Multimode 76-to-81GHz Automotive Radar Transceiver with Autonomous Monitoring," *ISSCC Dig. Tech. Papers*, pp. 158–159, Feb. 2018.

[8] Z. Li, P. Wang, R. Zeng, and W. Zhong, "Analysis of Wideband Multilayer LTCC Vertical Via Transition for Millimeter-wave System-in-package," in *18th International Conference on Electronic Packaging Technology (ICEPT)*, Aug. 2017, pp. 1039–1042.

[9] D. Pozar, *Microwave Engineering*, 4th ed. John Wiley and Sons, 2012.

[10] A. Carmona-Cruz, K. Scharff *et al.*, "Via Transition Optimization Using a Domain Decomposition Approach," in *IEEE 23rd Workshop on Signal and Power Integrity (SPI)*, Jun. 2019, pp. 1–4.